Liver International ISSN 1478-3223

BASIC STUDIES

Targeted disruption of Smad3 confers resistance to the development of dimethylnitrosamine-induced hepatic fibrosis in mice

Giovanni Latella[1], Antonella Vetuschi[2], Roberta Sferra[2], Valentina Catitti[1], Angela D'Angelo[1], Giuliana Zanninelli[1], Kathleen C. Flanders[3] and Eugenio Gaudio[4]

1 Department of Internal Medicine, GI Unit, University of L'Aquila, L'Aquila, Italy
2 Department of Experimental Medicine, University of L'Aquila, L'Aquila, Italy
3 National Cancer Institute, National Institutes of Health, Bethesda, MD, USA
4 Department of Human Anatomy, University of Roma 'La Sapienza', Rome, Italy

Keywords
chronic hepatitis – DMN-induced hepatitis – ECM – fibrosis – liver fibrosis – Smad proteins – TGF-β

Correspondence
Giovanni Latella, MD, Dipartimento di Medicina Interna e Sanità Pubblica, Divisione di Gastroenterologia, Epatologia e Nutrizione, Università degli Studi dell'Aquila, Piazza Salvatore Tommasi, 1 – Coppito, 67100 L'Aquila, Italy
Tel: +39 0862 434736
Fax: +39 0862 434761
e-mail: giolatel@tin.it

Received 6 August 2008
Accepted 28 January 2009

DOI:10.1111/j.1478-3231.2009.02011.x

Abstract

Background: Hepatic fibrosis is characterized by a progressive accumulation of fibrillar extracellular matrix (ECM) proteins including collagen, which occurs in most types of chronic liver diseases. Transforming growth factor-β (TGF-β)/Smad3 signalling plays a central role in tissue fibrogenesis, acting as a potent stimulus of ECM accumulation. *Aim:* To evaluate the potential protective role of Smad3 deficiency in the pathogenesis of liver fibrosis induced by dimethylnitrosamine (DMN) in Smad3 null mice. *Methods:* - Chronic hepatitis-associated fibrosis was induced in 13 Smad3 null and 13 wild-type (WT) mice by intraperitoneal DMN administration (10 μg/g body weight/day) for three consecutive days per week for 6 weeks. The liver was excised for macroscopic examination and histological, morphometric and immunohistochemical (IHC) analyses. For IHC, α-smooth muscle actin (α-SMA), collagen types I–III, TGF-β1, connective tissue growth factor (CTGF), Smad3, Smad7 and CD3 antibodies were used. *Results:* At macroscopic examination, the liver of DMN-treated Smad3 WT appeared harder with a dark brown colouring and necrotic areas compared with that from null mice. Histological and morphometric evaluation revealed a significantly higher degree of hepatic fibrosis and accumulation of connective tissue in the Smad3 WT compared with null mice. IHC evaluation showed a marked increase in α-SMA, CTGF, collagen I-III, TGF-β and Smad3 staining in the liver of Smad3 WT compared with that in null mice, whereas Smad7 was increased only in null mice. *Conclusions:* The results indicate that Smad3 loss confers resistance to the development of DMN-induced hepatic fibrosis. The reduced fibrotic response appears to be due to a reduction of fibrogenic myofibroblast activation and ECM production and accumulation. Smad3 could be a novel target for potential treatment of fibrosis complicating chronic hepatitis.

Liver fibrosis is a progressive and excessive accumulation of fibrillar extracellular matrix (ECM) proteins that occurs during chronic liver tissue damage. Fibrosis is a common response to chronic liver diseases because of infective [mostly hepatitis C virus (HCV) and hepatitis B virus (HBV)], toxic/drug-induced, metabolic and autoimmune causes (1–3). The accumulation of ECM protein deranges the hepatic architecture by forming a fibrous scar, and the subsequent development of nodules of regenerating hepatocytes defines liver cirrhosis. Fibrosis is currently considered an abnormal wound-healing response to chronic liver injury. Fibrosis is a chronic and progressive process acting through complex cell/matrix/cytokine and growth factor interactions, but may be a reversible event (1–7). The cellular and molecular mechanisms underlying wound healing and fibrosis still remain to be fully elucidated.

Physiological fibrogenesis is initiated by parenchymal cell destruction owing to multiple harmful agents and mechanisms, followed by inflammation, which, in turn, activates 'resting' ECM-producing cells to produce and secrete ECM molecules, cytokines, chemokines, matrix metalloproteinases (MMPs) and their specific inhibitors [tissue inhibitors of metalloproteinases (TIMPs)] (1–6, 8, 9). Activated ECM-producing cells participate both in fibrogenesis and in fibrinolysis (degradation of ECM), and thus in tissue remodelling. Fibrogenesis may lead either to tissue repair or to fibrosis depending on the balance between ECM synthesis and degradation (1–6, 8, 9). After an acute liver injury, parenchymal cells

regenerate and replace the necrotic or apoptotic cells, a process associated with a limited deposition of ECM proteins. During a chronic injury, the liver regeneration may fail and hepatocytes are substituted with abundant ECM, including fibrillar collagen. Liver fibrosis is associated with both quantitative and qualitative changes of ECM. The collagenous and non-collagenous components increase three- to six-fold, accompanied by a shift from the normal low-density basement membrane-like matrix to an interstitial-type matrix containing fibrillar collagens (I–III) (2, 3).

Fibrosis shows different spatial patterns depending on the prevalent mechanisms and causes of tissue damage (1–3). Fibrosis that develops in chronic viral infection and chronic cholestatic disorders is initially concentrated within and around the portal tracts, while fibrosis secondary to toxic and metabolic damage is mainly located in the centrolobular areas. Different cell types are involved in the deposition of fibrillar ECM protein including collagen during hepatic fibrogenesis (1–5, 10). Hepatic stellate cells (HSCs) have a predominant role when tissue damage prevails within the liver lobule, whereas portal fibroblasts and myofibroblasts are involved when the damage is located in the portal tracts. Bone marrow-derived stromal cells recruited at the sites of liver injury may contribute to the population of fibrogenic cells (11). As a consequence of chronic tissue damage, ECM-producing cells, especially HSC, undergo a process of activation characterized by proliferation, motility, contractility and synthesis of ECM proteins.

Activation of ECM-producing cells is regulated by several soluble factors, including cytokines, chemokines, growth factors and products of oxidative stress (1, 5, 6, 8). Of these molecules regulating the activation of ECM-producing cells, transforming growth factor-β (TGF-β) appears to play a pivotal role (12–14). TGF-β is a member of a large family of pleiotropic cytokines that includes bone morphogenetic proteins (BMPs), activins and other related factors. Three different isoforms of TGF-β (β1, β2 and β3) have been found in mammals and TGF-β1 is the most extensively studied. The TGF-β intracellular signal transduction pathway is mediated mainly by Smad proteins (15, 16).

Smads are a family of eight related proteins that function as signalling intermediates for the TGF-β superfamily members (15, 16). Upon ligand binding and activation of TGF-β receptors (I, II and III), phosphorylated Smad2 and 3 bind with the common mediator Smad4. The Smad2/3–Smad4 complex translocates into the nucleus, where it regulates specific TGF-β target genes. The inhibitory Smad7 antagonizes TGF-β signalling by competing with ligation of Smad2/3 to the activated receptor complex Smad4. Specifically, the target genes known to contain Smad-responsive regions and that are directly or indirectly involved in fibrogenesis include several fibrillar ECM proteins (collagen, fibronectin), matrix-degrading enzymes (MMPs) and some specific inhibitors (plasminogen activator inhibitor type 1, TIMP-1), as well as genes regulating epithelial–mesenchymal cell transition, proliferation (cyclin-dependent kinase inhibitor p21) and apoptosis (caspases) (16, 17).

Besides its immune-regulatory function, TGF-β/Smads signalling also plays a central role in tissue fibrogenesis by acting as a potent stimulus of ECM protein accumulation (8, 12). Disruption of the TGF-β/Smads signalling pathway, either through the loss of Smad3 or the increase of Smad7 expression, confers resistance to tissue fibrosis in several organs including the skin, kidney, liver, lung and cardiovascular system (18–28). Schnabl *et al.* (20) have previously assessed the role of Smad3 in the activation of HSCs and expression of collagen type I in a model of acute liver injury *in vivo* and in culture-activated HSCs. Wild-type (WT), Smad3 heterozygous or homozygous knockout mice were treated with a single intragastric administration of CCl_4. Mice were sacrificed 72 h later. The authors showed, both *in vivo* and *in culture*, that Smad3 is not required for the activation process of HSCs, while it is required for the maximal induction of type I collagen expression (20).

The aim of the present study was to evaluate *in vivo* the role of Smad3 in the hepatic fibrogenesis in a model of chronic liver injury induced by an intraperitoneal administration of dimethylnitrosamine (DMN) in WT and Smad3 null mice.

Materials and methods

Animals

Colonies of Smad3 WT, heterozygous and null mice (Black Swiss × 129SVJ strain) were developed in our animal facility using pairs of Smad3 heterozygous mice kindly provided by A. Roberts (NCI, Bethesda, MD, USA). $Smad3^{ex8/ex8}$ mice were generated by targeted disruption of exon 8 in the Smad3 gene by homologous recombination (29).

All mice were maintained in a specific pathogen-free facility and routinely monitored. Mice were kept in micro-isolator cages and allowed free access to food and water. Mouse tail DNA was extracted and genotype analysis was performed using the polymerase chain reaction method as described previously (30, 31).

Overall, 40 healthy adult mice, 10 weeks of age, were included in this study: 20 Smad3 WT (seven controls, 13 receiving DMN) and 20 Smad3 null mice (seven controls, 13 receiving DMN).

The study protocol was approved by the Animal Research Committee of the University of L'Aquila, L'Aquila, Italy.

Induction of hepatitis

Chronic hepatitis-associated fibrosis was induced in 13 Smad3 null and 13 WT mice by intraperitoneal administration of DMN (Sigma Aldrich, Milan, Italy) under light ether anaesthesia. Each mouse received 10 μg DMN per

gram of body weight (1% in saline solution) for the first three consecutive days of the week for 6 weeks (32) (Fig. 1). Animals in the control groups (seven Smad3 WT and seven null mice) received a sham intraperitoneal injection of the same volume of 0.9% saline.

Animals were monitored daily for food and fluid intake and examined for signs of hepatitis including weight loss and abdominal distension caused by ascites (33) as well as signs of systemic inflammation such as piloerection, lethargy and peri-orbital exudates (34). Animals were weighed at the beginning of the study (pretreatment), and thereafter weekly before each DMN administration. Three days after the last DMN administration (post-treatment), the animals of each group underwent a laparotomy and were sacrificed by cervical dislocation under deep CO_2 anaesthesia.

For this protocol, the authors adhered to the Italian National Research Council criteria for the care and use of laboratory animals.

Sample recovery and preparation

Of the 40 mice included in the study, 33 survived and completed the experimental protocol: 17 Smad3 WT mice (seven controls and 10 DMN-treated mice) and 16 Smad3 null mice (seven controls and nine DMN-treated mice). Laparotomy was performed under anaesthesia, the liver was rapidly excised as a whole, weighted and placed in a Petri dish containing sterile saline solution. The presence of ascites (0 = absent, 1 = mild and 2 = severe) and adhesions (0 = absent, 1 = mild/focal-zonal and 2 = severe/diffuse) between the liver and adjacent organs was scored on a 0–2 scale. The right lobes of the liver were then fixed in 4% buffered formaldehyde and embedded in paraffin for histological studies [haematoxylin and eosin (H&E)] and Sirius red–fast green stain and immunohistochemistry).

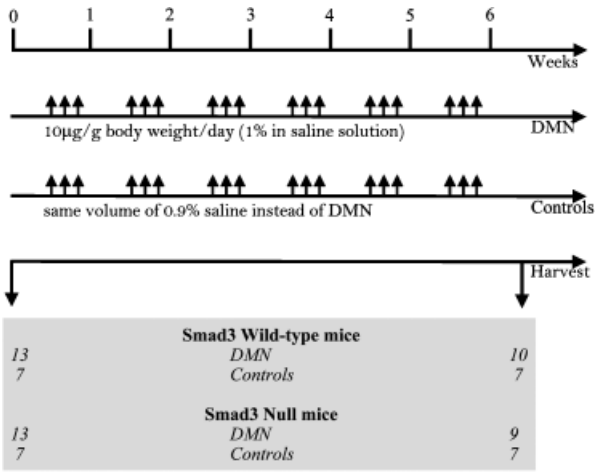

Fig. 1. Protocol of intraperitoneal dimethylnitrosamine (DMN) administration in Smad3 wild-type and null mice. Under light ether anaesthesia, mice received 10 μg DMN per gram of body weight (1% in saline solution) for the first three consecutive days of the week for 6 weeks. Animals in the control groups received an intraperitoneal injection of the same volume of 0.9% saline instead of DMN.

Analytical methods for serum samples

Blood samples were obtained from the inferior vena cava. Serum was collected from the blood sample by immediate centrifugation at 10 000*g* for 8 min at 4 °C. Serum alanine aminotransferase (ALT) and aspartate aminotransferase (AST) levels were measured by automated techniques. Serum levels of tumour necrosis factor-α (TNF-α) were determined by an enzyme-linked immunosorbent assay (ELISA) (mouse TNF-α, n. MTA00; R&D Systems Co. Ltd, Minneapolis, MN, USA).

Assessment of macroscopic and microscopic hepatic lesions

Two independent observers, unaware of either the mice genotype or the DMN treatment, scored the following parameters: liver appearance and colour (0 = physiologic, 1 = pathologic without necrosis and 2 = pathologic with necrosis), liver weight, liver weight/body weight ratio, spleen weight and spleen/body weight ratio.

Specimens obtained from the right lobe of the liver of all animals were washed and immediately immersed in 10% buffered formalin in phosphate-buffered saline (PBS) (pH 7.4) for 3 h at room temperature, followed by the standard procedure for paraffin embedding. Serial 3 μm sections were stained with H&E to assess the degree of inflammation and with Sirius red–fast green stain to detect connective tissue and fibrosis. The stained sections were then observed under an Olympus BX51 Light Microscope (Olympus, Optical Co. Ltd, Tokyo, Japan). Two pathologists (A. V. and R. S.), blinded to the study procedures, examined and scored all histological sections of the hepatic samples. Liver fibrosis and necro-inflammatory activity were evaluated semiquantitatively according to the METAVIR scoring system (35). Fibrosis was staged on a 0–4 scale as follows: F0 = no fibrosis; F1 = portal fibrosis without septa; F2 = numerous septa without cirrhosis; and F4 =cirrhosis. Necro-inflammatory activity was graded as follows: A0 = none; A1 = mild; A2 = moderate; and A3 severe.

Colorimetric evaluation of collagen content

Samples (5 mm^3) of the right lobe of the liver parenchyma, not including the Glisson's capsule and larger portal branches, were removed and immediately immersed in 10% buffered formalin for paraffin embedding. Eight 15-mm-thick, 100 mm^2 large sections were obtained from each liver and used for colorimetric evaluation. Additional 5-mm-thick sections were stained and observed by light microscopy together with stained sections for colorimetric evaluation according to Lopez-De Leòn and Rojkind (36).

Sections for colorimetric evaluation were deparaffinized through successive baths in absolute toluol, toluol:ethanol (50:50) and 50% aqueous ethanol and water. Staining procedures with fast green FCF 0.1 (no. IA30l; Chroma-Gesellschaft, Stuttgart, Germany) and Sirius red F3B 0.01% (no. 10022; Atomergic Chemical Corporation, Plainview, NY, USA) were performed according to Gascon-Barrè *et al.* (37). Colours were eluted in 0.05 M NaOH and 50% aqueous methanol.

The eluted colours were examined in a Lambda 4 B PE spectrophotometer (Perkin Elmer, Waltham, MA, USA). Correlations between absorbance and protein estimations were carried out according to Gascon-Barrè *et al.* (37).

Non-collagenous protein determination was performed using the following formula:

$$\text{Non-collagenous protein (mg)} = \text{absorbance at 605 nm}/2.08$$

Collagenous protein determination was obtained using the latter interference factor in the following formula:

$$\text{Collagen (mg)} = (\text{absorbance at 540 nm} - 0.26\,\text{absorbance at 605 nm})/38.4$$

Collagen content (collagen/protein ratio) was calculated using the following formula:

$$\text{Collagen content (mg/mg total protein)} = \text{mg collagen}/(\text{mg collagen} + \text{mg non-collagenous protein})$$

The above-mentioned formulae were applied according to Gascon-Barrè *et al.* (37).

Immunohistochemistry analysis

Samples of the right lobe of the liver were promptly fixed with 10% buffered formalin in PBS (pH 7.4) for 3 h, dehydrated in graded ethanol and embedded in a low-temperature-fusion paraffin. Serial 3 μm sections were incubated for 40 min in methanol and 3% hydrogen peroxide solution and then rinsed in PBS. Thereafter, sections were incubated overnight at 4 °C with polyclonal antibodies to CD3, α-smooth muscle actin (α-SMA), collagen types I–III, TGF-β1, Smad3, Smad7 and connective tissue growth factor (CTGF) (Santa Cruz Biotechnology Inc., Santa Cruz, CA, USA), used at a dilution of 1:100, 1:200, 1:200, 1:200, 1:100, 1:100, respectively, in PBS. Samples were then rinsed with PBS for 5 min and incubated with a labelled streptavidin–biotin–peroxidase conjugate kit (Dako LSAB, cod. K0675; Dako-Cytomation, Milan, Italy). After rinsing in PBS for 10 min, the sections were incubated with 3,3-diaminobenzidine-tetrahydrochloride (Sigma Aldrich, Milan, Italy) for 1–3 min.

For negative controls, the primary antibody was replaced (same dilution) with normal serum from the same species.

Finally, the samples were counterstained with Mayer's haematoxylin and observed under a photomicroscope (Olympus BX51 Light Microscopy) (Olympus, Optical Co. Ltd). The immunohistochemistry analysis was performed using the semiquantitative score, as described previously (38).

Statistical analysis

Statistical analyses were performed using Student's *t*-test, Fisher's exact test and the Mann–Whitney *U*-statistic test, when appropriate. Results were expressed as means ± standard deviation (SD). Probability values and confidence intervals (CI) were calculated at the 95% level. A *P*-value < 0.05 was considered statistically significant.

Results

Clinical and macroscopic findings

Smad3 null mice survived into adulthood, and, although at 5 weeks of age they were smaller than their WT littermates, they did not generally show any signs of wasting syndrome during the experimental period. Smad3 null mice always showed a lower body weight compared with the WT mice, apart from DMN treatment (Fig. 2). At the end of the treatment, the Smad3 WT mice receiving DMN had a lower body weight compared with the WT controls (21.60 ± 3.72 and 24.83 ± 3.03, respectively, $P < 0.05$), whereas no significant difference was observed between DMN-treated and control null mice (18.89 ± 3.26 and 18.25 ± 3.20, respectively, $P < 0.7$). Systemic manifestations, such as piloerection, peri-orbital

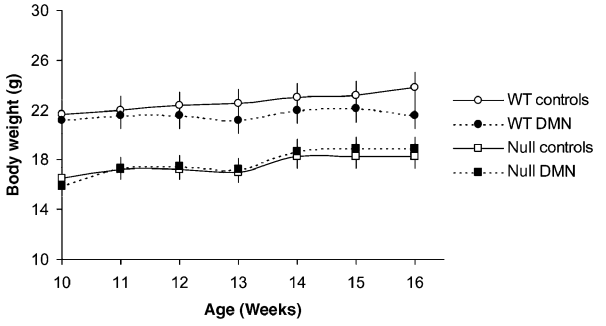

Fig. 2. Body weight gain curves of Smad3 wild-type (WT) and null groups of mice [controls and dimethylnitrosamine (DMN)], basal and weekly, over a 6-week treatment. Plot of weight (g) vs age (days). Each point represents mean weight data pooled from all mice in each group. Standard deviations are indicated. Each point between WT controls and null controls, as well as between WT DMN and null DMN, was statistically significant ($P < 0.001$). Comparing WT controls vs WT DMN, the difference was statistically significant only at the end of DMN treatment ($P < 0.05$), whereas no significant differences were observed between null controls and null DMN.

exudates and/or lethargy, were observed in 10% of WT and 20% of null mice between 2 and 4 weeks of DMN treatment.

Representative examples of liver taken from controls and DMN-treated Smad3 WT and null mice are shown in Figure 3. The liver of control Smad3 null mice was slightly smaller than that of control Smad3 WT (0.72 ± 0.15 and 1.06 ± 0.44, respectively, $P < 0.07$), without showing morphologic differences at the macroscopic evaluation. As compared with WT controls, DMN-treated WT mice had a darker colour of the liver and a marked thickness with a granulose appearance of the liver surface, accompanied, in several cases, by the presence of foci of necrosis, whereas the liver weight was not significantly different between the two groups of mice (0.82 ± 0.21 and 1.06 ± 0.44, respectively, $P < 0.1$). Smad3 null-treated and control mice did not show any significant difference in the above-mentioned parameters.

The effects of DMN administration on the course and macroscopic findings of hepatitis in DMN-treated Smad3 WT and null mice are outlined in Table 1. Age, sex and duration of DMN treatment were comparable in the two groups of mice. The mortality rates in Smad3 WT and null mice were 23% and 31% respectively. All deaths occurred within the first 3 weeks of treatment. Ascites was present in 40% of DMN-treated WT mice while adherences with other organs were present in 30%. DMN-treated null mice did not present ascites or adherences with adjacent organs. Figure 4 depicts the liver weight and liver weight/body weight ratio in both DMN-treated and control mice.

Microscopic findings

Representative histological findings (H&E and Sirius red–fast green stain) of the liver from Smad3 WT and null mice, either control or DMN-treated, are shown in Figures 5 and 6.

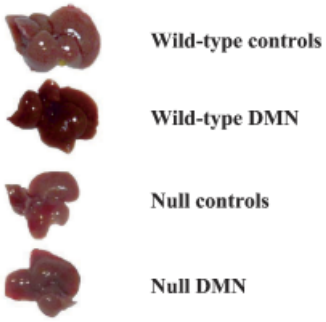

Fig. 3. Macroscopic appearance of the liver from Smad3 WT and null mice [controls and dimethylnitrosamine (DMN)]. The liver from DMN-treated Smad3 WT mice appeared smaller and harder and showed a more brown colouring with necrotic areas compared with that from WT controls. No difference was observed between the livers from DMN-treated Smad3 null and controls.

In the untreated control mice, histological assessment showed normal morphological patterns and a similar connective tissue distribution both in WT and in Smad3 null mice. In the portal biliary tracts of livers of Smad3 null mice, a mild reduction of connective tissue was observed, as compared with WT mice.

In the DMN-treated mice, histological evaluation showed marked changes in the structure of the liver from Smad3 WT mice (Figs 5 and 6). A marked increase of connective tissue in the portal tracts and within the liver parenchyma was found in Smad3 WT mice compared with null (Fig. 6). The degree of hepatic fibrosis was significantly higher in Smad3 WT compared with null mice (1.90 ± 0.56 vs 0.55 ± 0.53, respectively, $P < 0.0004$) (Table 2). The fibrosis stage (F) distribution in

Table 1. Effects of dimethylnitrosamine administration on course and macroscopic findings of hepatitis in Smad3 wild-type and null mice

Parameters	Wild-type ($n = 13$)	Null ($n = 13$)	P
Age (weeks)	10	10	NS
Sex (M/F)	11/2	8/5	NS
Duration of DMN treatment	6 weeks	6 weeks	NS
Mortality (*n* mice)	3	4	NS
Body weight (g)	21.60 ± 3.72	18.89 ± 3.26	NS
Ascites	0.50 ± 0.71	NP	NS
Adhesions	0.30 ± 0.48	NP	NS
Pathologic colouring	1.20 ± 0.42	0.11 ± 0.33	0.0003
Liver weight (g)	0.82 ± 0.21	0.74 ± 0.21	NS
Liver weight/body weight ratio	0.039 ± 0.013	0.038 ± 0.006	NS
Spleen weight (g)	0.11 ± 0.02	0.09 ± 0.04	NS
Spleen weight/body weight ratio	0.005 ± 0.001	0.004 ± 0.001	0.04

Data are expressed as mean ± SD.
NP, not present; NS, not significant.

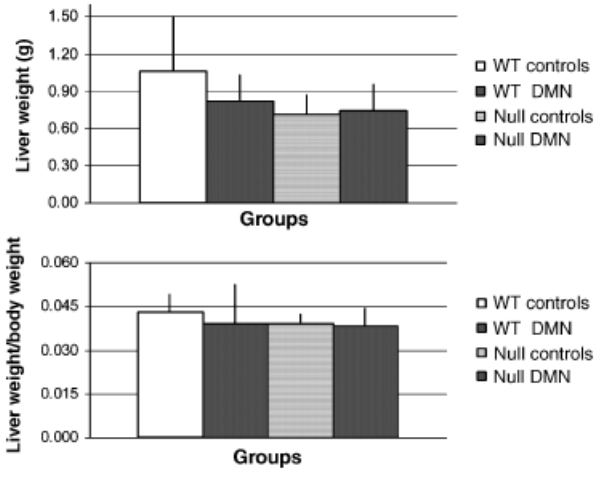

Fig. 4. Liver weight and liver weight/body weight ratio (%) in the four groups of mice.

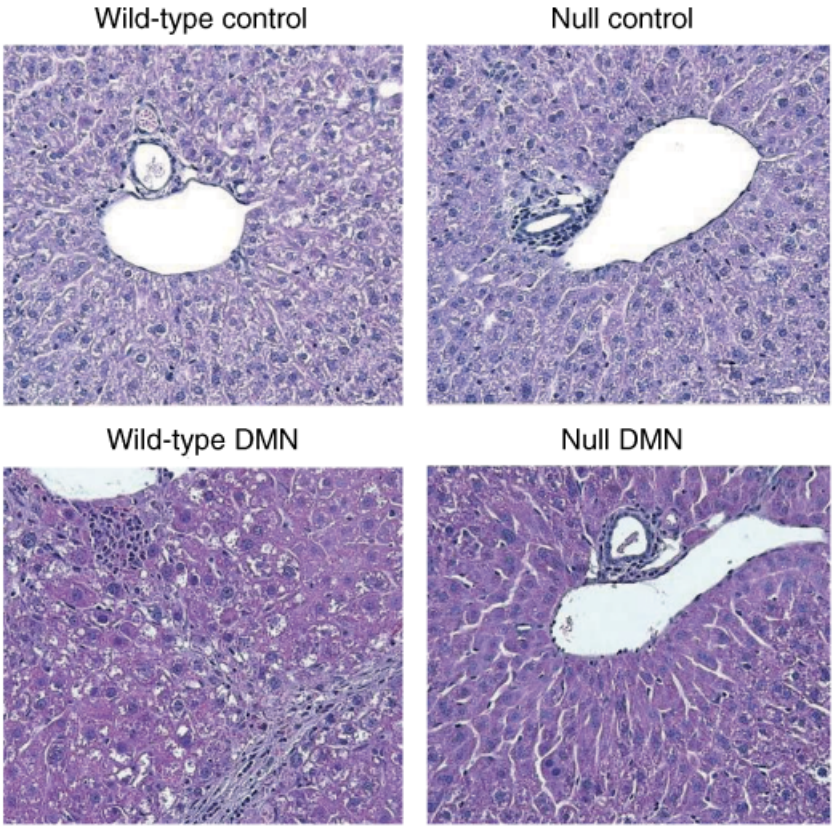

Fig. 5. The liver in the two control groups of mice is normal. Following dimethylnitrosamine (DMN) treatment, only a slight increase of inflammation is present in Smad3 WT compared with null mice. Haematoxylin–eosin staining, × 4.

Smad3 WT mice was as follows: F0-0/10, F1-2/10 (20%), F2-7/10 (70%), F3-1/10 (10%) and F4-0/10. In contrast, only 5/9 (44%) null mice developed a mild fibrosis (F1). Accordingly, colorimetric evaluation of collagen content demonstrated statistically higher values of collagen in the liver of Smad3 WT compared with null mice (Table 2). The degree of hepatic inflammation did not differ between the two groups of mice (0.60 ± 0.51 vs 0.55 ± 0.53, respectively, $P < 0.9$). Furthermore, both WT and null DMN-treated mice did not show significant differences in the serum levels of ALT (147.25 ± 93.54 vs 162.50 ± 97.12 U/L, respectively, $P = 0.73$), AST (451.00 ± 151.93 vs 509.00 ± 223.78 U/L, respectively, $P = 0.51$) and TNF-α (13.18 ± 3.24 vs 15.19 ± 4.21 ng/L, respectively, $P = 0.25$)

Immunohistochemical evaluation

In the untreated control mice, α-SMA and CTGF staining did not differ between the WT and null mice, whereas collagen I–III staining was slightly more intense in WT (data not shown). In the liver of Smad3 null mice, a clear increase in CD^{3+} T cells and TGF-β1 staining was observed compared with the liver of the WT mice (data not shown). Smad3 staining, absent in Smad3 null mice, was clearly present in the liver of WT mice. Smad7 staining was similar in the two groups of mice.

In the DMN-treated mice, α-SMA, collagen I–III, CTGF and TGF-β1 staining was markedly increased in Smad3 WT mice compared with null mice (Figs 7 and 8). Smad3 staining, absent in null mice, was increased in WT mice, whereas Smad7 staining was lower in WT mice compared with null mice (Fig. 8). CD^{3+} T cell staining was slightly increased in the liver of WT, compared with null mice (data not shown). Both TNBS-treated groups presented marked CD^{3+} T cell staining compared with untreated control mice.

Discussion

Hepatic fibrosis, responsible for structural and functional derangement within the liver, is present in several chronic liver diseases (1–3). At present, the lack of active antifibrotic drugs on both the prevention and the treatment of liver fibrosis is partly because of a poor understanding of the cellular and molecular mechanisms underlying fibrogenesis (1–3, 5, 6). During the past few years, *in vivo* studies on animal models of liver fibrosis and *in vitro* culture on HSC unravelled important fibrogenesis pathways at cellular and molecular levels (5,

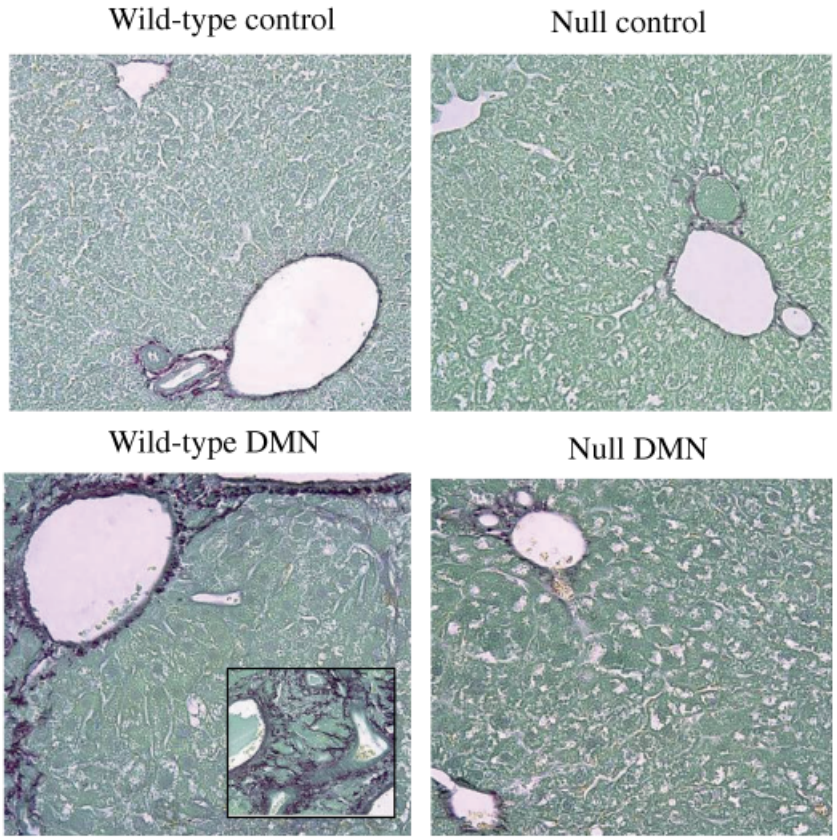

Fig. 6. Connective tissue distribution is similar in the two groups of control mice. Following dimethylnitrosamine (DMN) treatment, the liver from Smad3 wild-type shows a marked increase in the collagen content compared with that from DMN-treated null mice. Sirius red–fast green stain staining, $\times 4$.

Table 2. Degree of fibrosis and collagen content in the liver of the four groups of mice

	Fibrosis						
Group of mice	F0	F1	F2	F3	F4	Total Score	Collagen content (μg/mg total protein)
WT Controls	7	0	0	0	0	0	0.0136 ± 0.0005
P						0.0001	0.0001
DMN-treated WT	0	2	7	1	0	1.90 ± 0.56*	0.0195 ± 0.0021†
Null Controls	7	0	0	0	0	0	0.0132 ± 0.0005
P						NS	NS
DMN-treated null	4	5	0	0	0	0.55 ± 0.53	0.0135 ± 0.0013

Liver fibrosis was evaluated semiquantitatively according to the METAVIR scoring system (34).
Liver collagen content was assessed by a colorimetric method (35, 36).
Data are expressed as mean $\pm$ SD.
*$P < 0.0004$ vs DMN-treated null mice,
†$P < 0.0001$ vs DMN-treated null mice.
DMN, dimethylnitrosamine; NS, not significant; WT, wild-type.

6, 8). In particular, studies on transgenic animal model allowed one to shed light on the role of specific molecules in tissue fibrosis. Among them, TGF-β and the newly identified Smad proteins play a pivotal role in fibrogenesis (5, 12, 22, 39). Several studies demonstrated that Smad3 null mice are resistant to tissue fibrosis in many organs (18–22). Previously, Schnabl *et al*. (20) have assessed the role of Smad3 in the hepatic fibrogenesis in a model of acute liver injury induced by a single intragastric administration of CCl_4. They showed, both *in vivo* and in culture, that Smad3 is required for the maximal induction of type I collagen expression, and

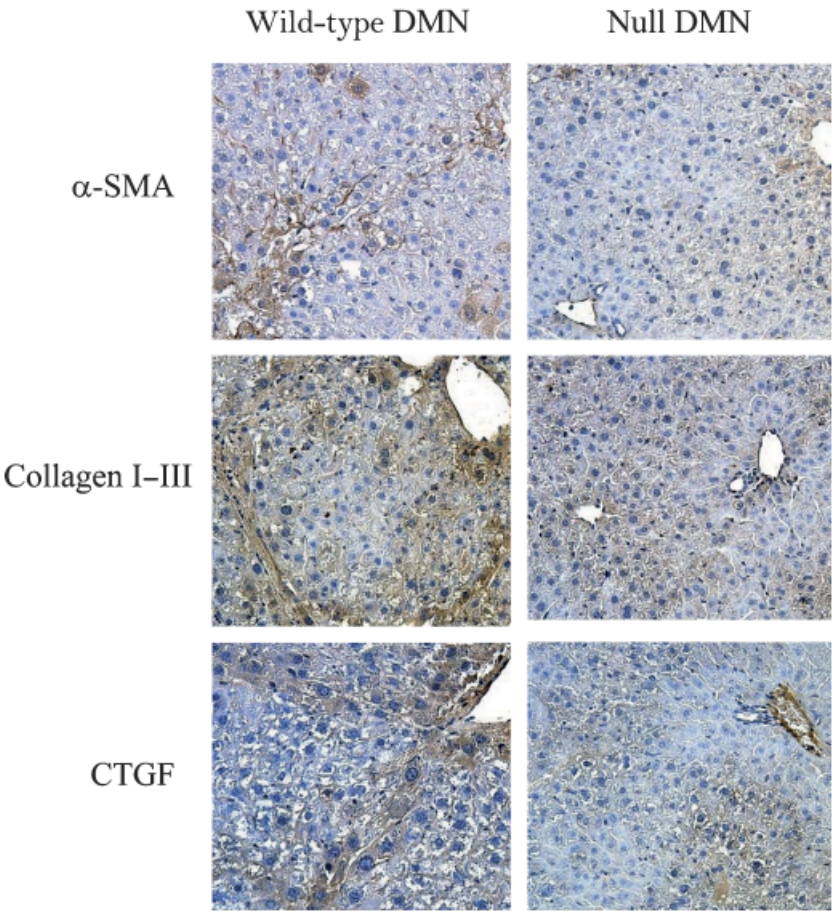

Fig. 7. α-smooth muscle actin (α-SMA), collagen I–III and connective tissue growth factor (CTGF) immunostainings are markedly increased in the liver from Smad3 wild-type compared with null dimethylnitrosamine (DMN)-treated mice. Immunohistochemistry, × 4.

that it is not essential for HSCs activation as assessed by α-SMA expression, but it is necessary for inhibition of HSCs proliferation. Current evidences suggest that the regulation of ECM production in acute and chronic liver injury are different (1–3, 40). ECM production is transient in acute liver disease, whereas it is sustained in chronic liver disease. Although different cell types may be involved in the ECM deposition, HSCs play a predominant role, at least in chronic injury. HSCs undergo a process of transdifferentiation from the quiescent 'fat-storing' phenotype to the 'myofibroblast-like' (MFBs) phenotype. Although the mechanisms controlling ECM production and accumulation have been broadly studied, the changes in the intracellular signals involved in the transdifferentiation of HSCs into MFBs have not yet been clarified. A differential regulation of TGF/Smad signals in HSCs has been reported during acute liver injury and MFBs during chronic liver injury (40). The different regulation of TGF/Smad signals following acute or chronic damage has also been documented in intestinal fibrogenesis (41).

The purpose of the present study was to evaluate the role of Smad3 in a model of chronic hepatitis-associated fibrosis. Therefore, we experimentally induced hepatic fibrosis in Smad3 WT and Smad3 null mice by an intraperitoneal injection of DMN for 6 weeks. DMN is a potent hepatotoxin that causes massive liver necrosis and a strong systemic inflammatory response (42). The regular low-dose injections exert a subacute and chronic hepatic damage with different degrees of necrosis and fibrosis (43). This experimental model mimics human hepatic fibrosis including its complications such as portal hypertension, ascites, hypoproteinaemia and abnormal values of biochemical parameters (44–47). Furthermore, the model has the advantage of inducing a reproducible fibrosis, progressive pathologic changes and a low degree of mortality among laboratory animals. We also performed a chronic low-dose CCl_4 treatment (administered by the intraperitoneal or the oral route) in mice two times a week; all the Smad3 null mice died after the third and fourth administration. The reason for this lethal effect of CCl_4 in Smad3 null mice is unclear, but is similar to that observed by Schnabl *et al.* (20). Therefore, we are unable to compare the effects of chronic CCl_4 and DMN in Smad3 null mice.

Following DMN treatment, Smad3 WT mice demonstrated a significant increase of hepatic fibrosis relative to

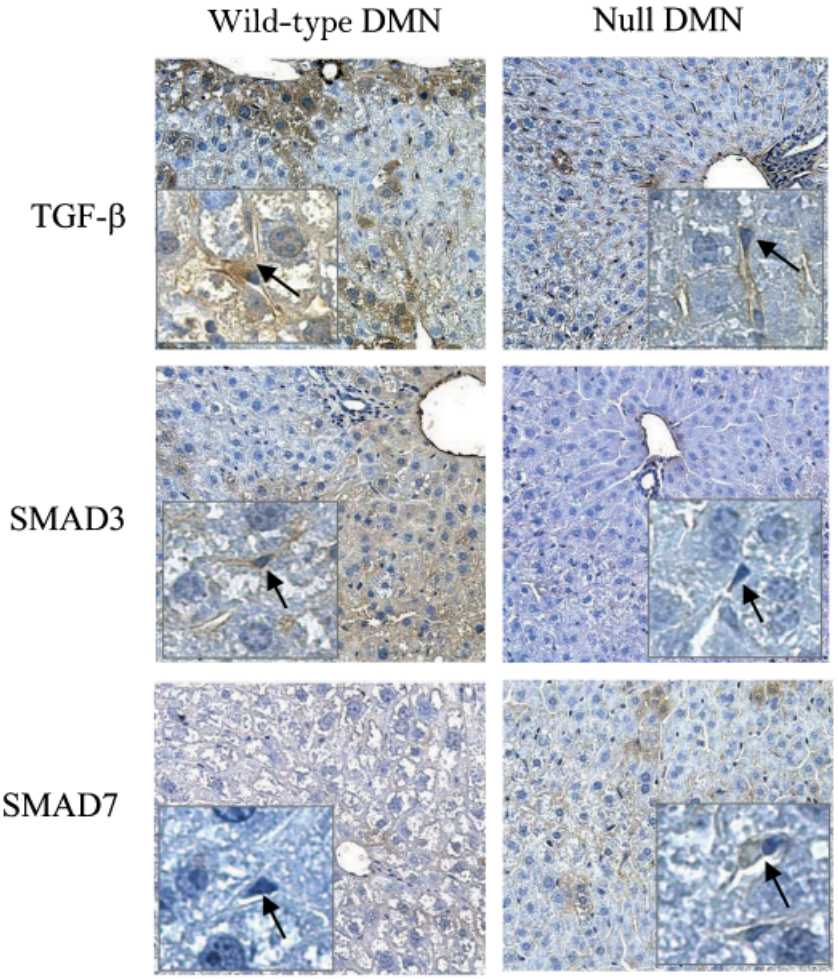

Fig. 8. Transforming growth factor-β1 (TGF-β1) immunostaining is most prominent in the liver from the wild-type (WT) as compared with null dimethylnitrosamine (DMN)-treated mice: immunohistochemistry × 4. Hepatic stellate cells (HSCs), the major source of collagen in the fibrotic liver, are positive both in WT and in null DMN-treated mice (indicated by arrows): immunohistochemistry × 40, inset. Smad3 immunostaining is markedly present in Smad3 WT and absent in null DMN-treated mice: immunohistochemistry × 4. At a higher magnification (× 40, inset), Smad3 positivity in HSCs of WT and absence in HSCs of null mice (indicated by arrows) are evident. Smad7 immunostaining is less prominent in Smad3 WT compared with that in null DMN-treated mice: immunohistochemistry, × 4 (inset, × 40, HSCs indicated by arrows).

that observed in Smad3 null at macroscopic and microscopic levels. As compared with WT controls, the liver of Smad3 WT DMN-treated mice presented a smaller size, a darker colour, a harder consistency of the parenchyma with a granular appearance and areas of necrosis and the presence of adherence to adjacent organs. These findings were absent in the liver of DMN-treated Smad3 null.

The histology, morphometry and immunohistochemistry evaluations of the liver of DMN-treated Smad3 WT mice demonstrated the presence of a significant amount of collagen deposition in pericellular tracts, in the space of Disse and around hepatic venules and portal tracts. In contrast, the liver of DMN-treated Smad3 null mice did not show any signs of parenchymal damage and the collagen distribution was comparable to that of controls. The absence of hepatic fibrosis in DMN-treated Smad3 null could not be attributed to a minor inflammation because the extent of liver damage and inflammatory infiltrate did not differ from that of DMN-treated WT mice. The blood ALT, AST and TNF-α levels did not differ in the two groups of mice. In contrast, only DMN-treated Smad3 WT mice developed hepatic fibrosis, consistent with the hypothesis that DMN-induced liver fibrosis is Smad3-dependent. These findings, observed in chronic DMN-induced hepatitis, are similar to those reported by Schnabl *et al*. (20) after an acute CCl_4-induced injury. After 72 h of CCl_4 administration, the degree of liver damage and inflammation, as well as TNF-α and interleukin-6 mRNA levels, were similar in Smad3 null and WT mice, whereas hepatic collagen mRNA was markedly lower in Smad3 null than WT mice.

Activated ECM-producing cells (myofibroblasts) play a central role in the pathogenesis of liver fibrosis (1–5). Immunohistochemical analysis of the liver of

DMN-treated Smad3 WT showed a higher tissue α-SMA expression relative to DMN-treated Smad3 null. α-SMA is a marker of ECM-producing cells activation, and overexpression of Smad3 itself is indeed responsible for the increase of expression and organization of α-SMA fibres, fibronectin and collagen type I deposition (2–5, 12, 48, 49). In the acute model of liver injury of Schnabl *et al.* (20), α-SMA expression increased after CCl_4 treatment to a similar extent at the site of parenchymal damage in Smad3 WT and null mice. The discrepancy in the α-SMA expression between our study and that of Schnabl and colleagues is not clear, but it could be due to the difference in the models used (CCl_4 vs DMN) and to the extent of the treatment (early vs late effects). It has been reported that α-SMA expression was significantly increased after 3–6 weeks of CCl_4 treatment, while it was unchanged after 36 h (40). In contrast to the transient activation of HSCs after acute liver injury, the activation process of HSCs transdifferentiation to MFBs seems to be sustained throughout chronic liver injury. Furthermore, it has been reported that Smad3-overexpressing cells demonstrated more focal adhesions and increased α-SMA organization in stress fibres indicating that Smad3 plays an important role in the morphological and functional maturation of hepatic MFBs (48).

Activated hepatic myofibroblasts may derive from different cell types such as myofibroblasts of the portal tracts, biliary epithelial cells and hepatocytes, bone marrow stem cells and mainly from HSC (1–5, 8, 11, 14). HSC normally reside in the space of Disse, but during an inflammatory process, they become phenotypically like a myofibroblast, acquiring proliferation, mobility and contractility properties. Once the transdifferentiation process starts, transformed myofibroblasts are capable of autocrine stimulation owing to a variety of secreted mediators and surface receptor expression. Myofibroblast activation may therefore become progressive and independent of inflammation, suggesting the hypothesis that inflammation is a necessary event to start the fibrotic response, but plays a minor role in the progression of the disease (41, 50). The fact that fibrosis in different organs does not respond to anti-inflammatory drugs corroborates the hypothesis that inflammation is not a key process in the pathogenesis and progression of the disease.

At present, hepatic fibrosis is considered a chronic progressive, dynamic and potentially reversible process (2, 3, 7). An important goal of research would be to identify antifibrotic agents capable of either inhibiting the accumulation of activated EMC-producing cells or their profibrogenic action, or capable of directly degrading EMC (1–5). Although many cytokines and growth factors are involved in fibrogenesis, experimental evidences suggest that the TGF-β/Smads pathway plays a predominant role in the disease by upregulating ECM expression and suppressing the matrix degradation via inhibition of MMPs (1–5, 8, 9, 12). Furthermore, TGF-β1 stimulates the synthesis of CTGF, a potent enhancer of fibroblast proliferation, ECM production and TGF-β self-induction (12, 50–54). Consistent with these findings, collagen I–III, CTGF and TGF-β1 staining in fibrotic liver tissue of Smad3 WT DMN-treated mice was markedly increased as compared with non-fibrotic liver tissue isolated from Smad3 null DMN-treated mice. Also, Smad3 expression, absent in Smad3 null mice, was considerably increased in DMN-treated Smad3 WT relative to controls. In contrast, DMN-treated Smad3 null presented a higher expression of Smad7 relative to DMN-treated Smad3 WT mice. Smad2 expression has not been assessed in this study. A differential regulation of TGF/Smad signals in ECM-producing cells has been reported during acute and chronic injury either of the liver or the large bowel (40, 41, 55). Smad2/3 and Smad7 seem to be inversely correlated during the acute and chronic phase of the experimentally induced inflammation. In the acute non-fibrogenic phase of inflammation, there is an increase of Smad7 expression paralleled by a decrease of Smad2/3. In contrast, the chronic fibrogenic phase is associated with higher Smad2/3 and lower Smad7 expression.

Several downstream pathways such as Smads or ERK/cJUN/p38 MAP kinases are activated by TGF-β superfamily members including activin, and they form a complex signalling network with extensive crosstalk (5, 6, 12, 15, 16, 22, 56, 57). The Smad signal transduction pathway is crucial in mediating several TGF-β responses in ECM-producing cells. Important Smad-dependent profibrotic effects of TGF-β include activation of myofibroblasts, stimulation of α-SMA, collagens, CTGF, TIMPs and plasminogen activator inhibitor type-1 and inhibition of MMPs (12, 16, 22). These transcriptional responses appear to be mediated primarily through Smad3, whereas the role of the other Smads has not yet been defined (12, 22, 48, 49, 58). Smad2 and 3, although structurally similar, are functionally distinct proteins that are phosphorylated at the C-terminal SSXS motif by the activated type I TGF-β receptor (16, 48, 59). Because Smad2, in contrast to Smad3, cannot bind to DNA directly, Smad2 and Smad3 may have a different subset of target genes and thus regulated distinct gene responses. Smad2 and Smad3 play different roles in quiescent and activated HSCs, particularly in matrix protein deposition, chemotaxis, cytoskeletal organization, contractility, matrix interactions and proliferation. Some of the responses induced by blocking Smad3 may be the result of altered activin signalling in addition to TGF-β signalling (57). A series of recent studies revealed important functions of activins, in particular of activin A, in tissue inflammation, repair and fibrosis of several organs including the liver (57).

Besides the TGF-β/Smad pathway, myofibroblasts also appear to play a role in liver fibrosis through the action of other fibrogenetic molecules, such as interleukin-1B, interleukin 13, insulin-like growth factor-1, TNF-α, CTGF, platelet-derived growth factor, basic fibroblast growth factor, angiotensin-converting enzyme,

angiotensin II, vascular endothelial growth factor, endothelin-1 and peroxisome proliferate-activated receptor-γ, which seem to interact directly with Smad3 or their activities are Smad3-dependent (5, 6, 12, 16, 22, 50).

A possible pathway to inhibit or prevent fibrosis could be that of blocking the TGF-β signal at the ligand and receptor extracellular level or at the intracellular level via signal transduction (5, 12, 22, 39, 54, 58). The inhibition of a single intracellular mediator may selectively block the fibrosis response of TGF-β without affecting other important or vital functions. The targeted disruption of TGF-β, Smad2 and Smad4 is lethal (60–62), while the Smad3 disruption results in viable mice until adulthood (29, 63, 64). Several experimental studies demonstrated that the disruption of the TGF-β/SMADs signalling, owing to loss of Smad3 or an increase of Smad7 expression, confers resistance to tissue fibrosis in many organs (18–28), finding also confirmed in liver fibrosis by the present study.

In conclusion, targeted disruption of Smad3 confers resistance to the development of liver fibrosis. The reduced fibrotic response appears to be due to a reduction of fibrogenic myofibroblast activation and ECM production and accumulation. Considering the prominent role of Smad3 in tissue fibrogenesis, its inhibition could constitute a valid and effective approach in the prevention and treatment of hepatic fibrosis.

Acknowledgements

The authors are grateful to the late Prof. AB Roberts (NCI, Bethesda, MD, USA) for providing the pairs of Smad3 heterozygous mice from which the Smad3 WT and null mice were obtained for the present study, Dr Romina Mancinelli for skilful technical assistance and Mrs Marian Shields for help in editing the manuscript.

Financial disclosure: None.

References

1. Friedman SL. Mechanisms of disease: mechanisms of hepatic fibrosis and therapeutic implications. *Nat Clin Pract Gastroenterol Hepatol* 2004; **1**: 98–105.
2. Pinzani M, Rombouts K, Colagrande S. Fibrosis in chronic liver diseases: diagnosis and management. *J Hepatol* 2005; **42**: S22–36.
3. Bataller R, Brenner DA. Liver fibrosis. *J Clin Invest* 2005; **115**: 209–18.
4. Powell DW, Mifflin RC, Valentich JD, *et al*. Myofibroblasts I. Paracrine cells important in health and disease. *Am J Physiol Cell Physiol* 1999; **277**: C1–19.
5. Gressner AM, Weiskirchen R. Modern pathogenetic concepts of liver fibrosis suggest stellate cell and TGF-β as major players and therapeutic targets. *J Cell Mol Med* 2006; **10**: 76–99.
6. Wynn T. Cellular and molecular mechanisms of fibrosis. *J Pathol* 2008; **214**: 199–210.
7. Desmet VJ, Roskams T. Cirrhosis reversal: a duel between dogma and myth. *J Hepatol* 2004; **40**: 860–7.
8. Iredale JP. Models of liver fibrosis: exploring the dynamic nature of inflammation and repair in a solid organ. *J Clin Invest* 2007; **117**: 539–48.
9. Arthur MJ. Fibrogenesis II. Metalloproteinases and their inhibitors in liver fibrosis. *Am J Physiol Gastrointest Liver Physiol* 2000; **279**: G245–9.
10. Reeves HL, Friedman SL. Activation of hepatic stellate cells – a key issue in liver fibrosis. *Front Biosci* 2002; **7**: d808–26.
11. Kisseleva T, Uchinami H, Feirt N, *et al*. Bone marrow-derived fibrocytes participate in pathogenesis of liver fibrosis. *J Hepatol* 2006; **45**: 429–38.
12. Inagaki Y, Okazaki I. Emerging insights into transforming growth factor β/smad signal in hepatic fibrogenesis. *Gut* 2007; **56**: 284–92.
13. Weng HL, Ciuclan L, Liu Y, *et al*. Profibrogenic transforming growth factor-beta/activin receptor-like kinase 5 signaling via connective tissue growth factor expression in hepatocytes. *Hepatology* 2007; **46**: 1257–70.
14. Kaimori A, Potter J, Kaimori JY, *et al*. Transforming growth factor-beta1 induces an epithelial-to-mesenchymal transition state in mouse hepatocytes in vitro. *J Biol Chem* 2007; **282**: 22089–101.
15. Shi Y, Massague J. Mechanisms of TGF-beta signaling from cell membrane to the nucleus. *Cell* 2003; **113**: 685–700.
16. Roberts AB, Russo A, Felici A, Flanders KC. Smad3: a key player in pathogenetic mechanisms dependent on TGF-beta. *Ann NY Acad Sci* 2003; **995**: 1–10.
17. Verrecchia F, Chu ML, Mauviel A. Identification of novel TGF-β/smad gene targets in dermal fibroblasts using a combined cDNA microarray/promoter transactivation approach. *J Biol Chem* 2001; **276**: 17058–62.
18. Lakos G, Tacagawa S, Chen SJ, *et al*. Targeted disruption of TGF-beta/Smad3 signaling modulates skin fibrosis in a mouse model of scleroderma. *Am J Pathol* 2004; **165**: 203–17.
19. Zhao J, Shi W, Wang YL, *et al*. Smad3 deficiency attenuates bleomycin-induced pulmonary fibrosis in mice. *Am J Physiol Lung Cell Mol Physiol* 2002; **282**: L585–93.
20. Schnabl B, Kweon YO, Frederick JP, *et al*. The role of Smad3 in mediating mouse hepatic stellate cell activation. *Hepatology* 2001; **34**: 89–100.
21. Inazaki K, Kanamaru Y, Kojima Y, *et al*. Smad3 deficiency attenuates renal fibrosis, inflammation, and apoptosis after unilateral ureteral obstruction. *Kidney Int* 2004; **66**: 597–604.
22. Flanders KC. Smad3 as a mediator of the fibrotic response. *Int J Exp Pathol* 2004; **85**: 47–64.
23. Fukasawa H, Yamamoto T, Togawa A, *et al*. Down-regulation of Smad7 expression by ubiquitin-dependent degradation contributes to renal fibrosis in obstructive nephropathy in mice. *Proc Natl Acad Sci USA* 2004; **101**: 8687–92.
24. Dooley S, Hamzavi J, Breitkopf K, *et al*. Smad7 prevents activation of hepatic stellate cells and liver fibrosis in rats. *Gastroenterology* 2003; **125**: 178–91.

25. Dong C, Zhu S, Wang T, *et al.* Deficient Smad7 expression: a putative molecular defect in scleroderma. *Proc Natl Acad Sci USA* 2002; **99**: 3908–13.
26. Nakao A, Fujii M, Matsumura R, *et al.* Transient gene transfer and expression of Smad7 prevents bleomycin-induced lung fibrosis in mice. *J Clin Invest* 1999; **104**: 5–11.
27. Tsai S, Ryer EJ, Kundy R, *et al.* Inhibition of TGF-beta signaling via Smad7 gene transfer decreases intimal hyperplasia after vascular injury. *J Surg Res* 2008; **144**: 216–7.
28. Wang B, Omar A, Angelovska T, *et al.* Regulation of collagen synthesis by inhibitory Smad7 in cardiac myofibroblasts. *Am J Heart Circ Physiol* 2007; **293**: H1282–90.
29. Yang X, Letterio JJ, Lechleider RJ, *et al.* Targeted disruption of Smad3 results in impaired mucosal immunity and diminished T cell responsiveness to TGF-beta. *EMBO J* 1999; **18**: 1280–91.
30. Ren Li M, Cai H, Hudgins S, Furth PA. A simplified method to prepare PCR template DNA for screening of transgenic and knockout mice. *Contemp Top Lab Anim Sci* 2001; **40**: 27–30.
31. Zanninelli G, Vetuschi A, Sferra R, *et al.* Smad3 knock-out mice as a useful model to study intestinal fibrogenesis. *World J Gastroenterol* 2006; **12**: 1211–8.
32. Yoshida T, Ogata H, Kamio M, *et al.* SOCS1 is a suppressor of liver fibrosis and hepatitis-induced carcinogenesis. *J Exp Med* 2004; **199**: 1701–7.
33. Luo YJ, Yu JP, Shi ZH, Wang L. *Ginkgo biloba* extract reverses CCl_4-induced liver fibrosis in rats. *World J Gastroenterol* 2004; **10**: 1037–42.
34. Hotchkiss RS, Swanson PE, Cobb JP, *et al.* Apoptosis in lymphoid and parenchymal cells during sepsis: findings in normal and T- and B-cell-deficient mice. *Crit Care Med* 1997; **25**: 1298–307.
35. Intraobserver and interobserver variations in liver biopsy interpretation in patients with chronic hepatitis C. The French METAVIR Cooperative Study Group. *Hepatology* 1994; **20**: 15–20.
36. Lopez-De Leòn A, Rojkind M. A simple micromethod for collagen and total protein determination in formalin-fixed paraffin embedded sections. *J Histochem Cytochem* 1985; **33**: 737–43.
37. Gascon-Barrè M, Huet PM, Belgiorno J, Plourde V, Coulombe PA. Estimation of collagen content of liver specimens. Variation among animals and among hepatic lobes in cirrhotic rats. *J Histochem Cytochem* 1989; **37**: 377–81.
38. Gaudio E, Barbaro B, Alvaro D, *et al.* Administration of r-VEGF-A prevents hepatic artery ligation-induced bile duct damage in bile duct ligated rats. *Am J Physiol Gastrointest Liver Physiol* 2006; **291**: G307–17.
39. Liu X, Hu H, Yin JQ. Therapeutic strategies against TGF-beta signaling pathway in hepatic fibrosis. *Liver Int* 2006; **26**: 8–22.
40. Tahashi Y, Matsuzaki K, Date M, *et al.* Differential regulation of TGF-beta signal in hepatic stellate cells between acute and chronic rat liver injury. *Hepatology* 2002; **35**: 49–61.
41. Fichtner-Feigl S, Fuss IJ, Young CA, *et al.* Induction of IL-13 triggers TGF-β1-dependent tissue fibrosis in chronic 2,4,6-trinitrobenzene sulfonic acid colitis. *J Immunol* 2007; **178**: 5859–70.
42. Hashimoto N, Ishikawa Y, Utsunomiya J. Effects of portacaval shunt, transposition and dimethylnitrosamine induced chronic liver injury on pancreatic hormones and amino acids in dog. *J Surg Res* 1989; **46**: 35–40.
43. George J, Rao KR, Stern R, Chandrakasan G. Dimethylnitrosamine-induced liver injury in rats: the early deposition of collagen. *Toxicology* 2001; **156**: 129–38.
44. George J. Mineral metabolism in dimethylnitrosamine-induced liver fibrosis. *Clin Biochem* 2006; **39**: 984–91.
45. Hu Q, Liu G. Effects of bicyclol on dimethylnitrosamine-induced liver fibrosis in mice and its mechanism of action. *Life Sci* 2006; **79**: 606–12.
46. George J, Chandrakasan G. Biochemical abnormalities during the progression of hepatic fibrosis induced by dimethylnitrosamine. *Clin Biochem* 2000; **33**: 563–70.
47. Jezequel AM, Mancini R, Rinaldesi ML, *et al.* Dimethylnitrosamine-induced cirrhosis. Evidence for an immunological mechanism. *J Hepatol* 1989; **8**: 42–52.
48. Uemura M, Swenson ES, Gaca MD, *et al.* Smad2 and Smad3 play different roles in rat hepatic stellate cell function and alpha-smooth muscle actin organization. *Mol Biol Cell* 2005; **16**: 4214–24.
49. Inagaki Y, Mamura M, Kanamaru Y, *et al.* Constitutive phosphorylation and nuclear localization of Smad3 are correlated with increased collagen gene transcription in activated hepatic stellate cells. *J Cell Physiol* 2001; **187**: 117–23.
50. Bonniaud P, Margetts PJ, Ask K, *et al.* TGF-ß and Smad3 signaling link inflammation to chronic fibrogenesis. *J Immunol* 2005; **175**: 5390–5.
51. Gressner AM, Yagmur E, Lahme B, Gressner O, Stanzel S. Connective tissue growth factor in serum as a new candidate test for assessment of hepatic fibrosis. *Clin Chem* 2006; **52**: 1815–17.
52. George J, Tsutsumi M. siRNA-mediated knockdown of connective tissue growth factor prevents *N*-nitrosodimethyllamine-induced hepatic fibrosis in rats. *Gene Ther* 2007; **14**: 790–803.
53. Li G, Xie Q, Shi Y, *et al.* Inhibition of connective tissue growth factor by siRNA prevents liver fibrosis in rats. *J Gene Med* 2006; **8**: 889–900.
54. Kim KH, Kim HC, Hwang MY, *et al.* The antifibrotic effect of TGF-beta1 siRNAs in murine model of liver cirrhosis. *Biochem Biophys Res Commun* 2006; **343**: 1072–8.
55. Latella G, Zanninelli G. Prevention and treatment of intestinal fibrosis: up-regulate smad7 or inhibit smad3 expression. *Eur J Clin Invest* 2008; **38**: 878–80.
56. Moustakas A, Helding CH. Non-Smad TGF-β signals. *J Cell Sci* 2005; **118**: 3573–84.
57. Werner S, Alzheimer C. Roles of activin in tissue repair, fibrosis, and inflammatory disease. *Cytokine Growth Factor Rev* 2006; **17**: 157–71.
58. Friedman SL, Rockey DC, Bissell DM. Hepatic fibrosis 2006: report of the third AASLD single topic conference. *Hepatology* 2007; **45**: 242–9.
59. Liu C, Gaca MD, Swenson ES, *et al.* Smad2 and 3 are differentially activated by transforming growth factor-beta

(TGF-beta) in quiescent and activated hepatic stellate cells. Constitutive nuclear localization of Smads in activated cells is TGF-beta-independent. *J Biol Chem* 2003; **278**: 11721–8.
60. Kulkarni AB, Huh CG, Becker D, *et al*. Transforming growth factor beta 1 null mutation in mice causes excessive inflammatory response and early death. *Proc Natl Acad Sci USA* 1993; **90**: 770–4.
61. Nomura M, Li E. Smad2 role in mesoderm formation, left-right patterning and craniofacial development. *Nature* 1998; **393**: 786–90.
62. Yang X, Li C, Hu X, Deng C. The tumor suppressor Smad4/DPC4 is essential for epiblast proliferation and mesoderm induction in mice. *Proc Natl Acad Sci USA* 1998; **95**: 3667–72.
63. Datto MB, Frederick JP, Pan L, *et al*. Targeted disruption of Smad3 reveals an essential role in transforming growth factor beta-mediated signal transduction. *Mol Cell Biol* 1999; **19**: 2495–504.
64. Zhu Y, Richardson JA, Parada LF, Graff JM. Smad3 mutant mice develop metastatic colorectal cancer. *Cell* 1998; **94**: 703–14.